GEOPHYSICAL RESEARCH LETTERS, VOL. 12, NO. 9, PAGES 557-560, SEPTEMBER 1985

SAWTOOTH SEGMENTATION AND DEFORMATION PROCESSES ON THE SOUTHERN SAN ANDREAS FAULT, CALIFORNIA

Roger Bilham[1] and Patrick Williams[2]

Lamont Doherty Geological Observatory of Columbia University

Abstract. Five contiguous 12-13 km fault segments form a sawtooth geometry on the southernmost San Andreas fault. The kinematic and morphologic properties of each segment depend on fault strike, despite differences of strike between segments of as little as 3 degrees. Oblique slip (transpression) of fault segments within the Indio Hills, Mecca Hills and Durmid Hill results from an inferred 8:1 ratio of dextral slip to convergence across the fault zone. Triggered slip and creep are confined almost entirely to transpressive segments of the fault. Durmid Hill has been formed in the last 28 ± 6 ka by uplift at an average rate of 3 ± 1 mm/a.

Introduction

A possible magnitude for a future earthquake on the San Andreas fault south of the Transverse Ranges (Figure 1) has been estimated to be $7.6 < Mw < 7.8$ with a recurrence interval of between 160 and 360 a [Sykes and Nishenko, 1984]. We have no reliable data to indicate the occurrence of an earthquake in the past century but prehistoric events have been revealed in trenches across the fault near Indio (Sieh, personal communication, 1985). The average creep rate [Louie et al., 1985] in the Coachella Valley (≈2 mm/a) is an order of magnitude less than the dextral displacement observed geodetically across the valley (>20 mm/a) [Savage, 1983; King and Savage, 1983]. Despite the absence of an historic earthquake, the trace of the San Andreas fault in the Coachella Valley is marked in several locations by fresh-looking scarps. Cracks attributable to triggered slip [Allen et al., 1972; Sieh, 1982], a form of aseismic accelerated fault creep, appeared along part of the fault zone within hours of the occurrence of the Borrego Mountain earthquake of 1968 and the Imperial Valley earthquake of 1979 (Figure 1). Although the mechanism of triggered slip remains obscure [Fuis, 1972] its spatial distribution correlates well with the geometry of the fault zone.

Fault Zone Geometry

We digitized the elevation (±0.3 m) and location (±2.5 m) of the fault trace at 100-m intervals along the mapped trace of the San Andreas fault in the Coachella Valley [Clark, 1984]. The fault consists of three approximately straight segments with remarkably similar strike (N47.5W) associated with high ground, separated by two right-stepping segments where the fault is at lower elevation (Figure 2). Each of the segments has a similar 12.3 ± 0.3 km length and along each segment the mean deviation of mapped fault strands from a straight line is less than 0.3% of the length of the segment (Table 1). If larger segments of the fault than those tabulated in Table 1 are examined, the deviation of the fault trace from the least-squares fit exceeds the 60-m (3σ) mean deviation computed for the entire segment. The straightness and similarity of the lengths of each of the segments results in a simple sawtooth geometry to the fault zone. The 12-km scale of fault segmentation is comparable to the depth of the deepest seismic events associated with the San Andreas fault zone in the Coachella Valley. Wallace [1973] noted a similar relationship in central California.

Several physical characteristics of the fault are related directly to fault strike (Figure 2). Triggered slip [Allen et al., 1972] is almost exclusively confined to the N47.5W striking Mecca Hills and Durmid Hill segments (Figure 2(c) and (d)). Recent sedimentary rocks are uplifted and folded by oblique slip transpression [Sylvester and Smith, 1976; Sanderson and Marchini, 1984] and fault zone morphology is pronounced [Sharp,

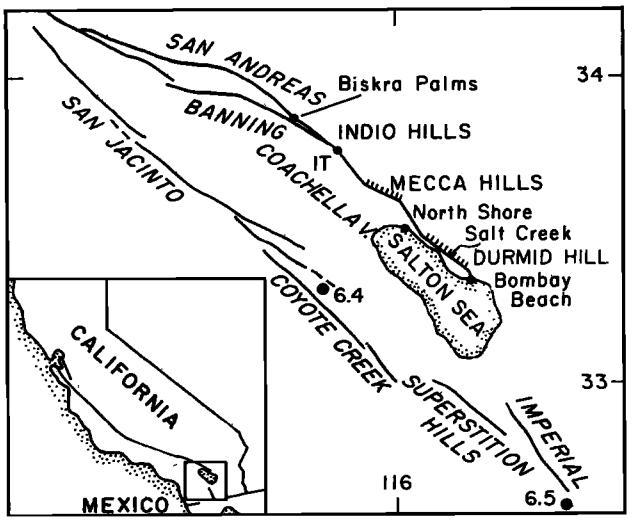

Fig. 1. Location of the Coachella Valley section of the southern San Andreas fault. The 72-km long section between Biskra Palms and Bombay Beach (enlarged in Fig. 2(a)) includes five straight segments, two of which slipped (hatched line) soon after the M = 6.4 Borrego Mountain (1968) and M = 6.5, Imperial Valley (1979) earthquakes. IT = Indio trench of K. Sieh.

[1]1985-86 Visiting Fellow, Joint Institute for Laboratory Astrophysics, University of Colorado and National Bureau of Standards, Boulder, CO 80309.

[2]Department of Geological Sciences of Columbia University, New York.

Paper number 5L6613.
0094-8276/85/005L-6613$03.00

TABLE 1. Geometric properties of the southern San Andreas fault in the Coachella Valley (33°47' to 33°23'N)

Segment	Length ±200 m (km)	Strike ±0.15° (N-W)	Standard deviation (m)	Average triggered slip (mm)		Observed creep rate (mm/a)
				1968	1979	
Indio Hills	12	48.09	±20	---	---	2
Canal	12.0	43.78	±25	---	---	---
Mecca Hills	12.6	47.42	±30	9.5	4	3
North Shore	12.6	40.36	±20	0.05	---	0
Durmid Hill	12.6	47.48	±25	5	2.5	2

Standard deviation is from a least-squares fit to all mapped fault strands in each segment. A standard deviation is calculated for the southern 7 km only of the Indio Hills segment which is much fragmented north of its inferred intersection with the Banning fault. Segment length is determined by the intersection of least-squares fit straight lines from adjacent segments. The numerical values for triggered slip are calculated by dividing the sum of the maximum observed slip [Allen et al., 1972; Sieh, 1982] in each 1-km section of the fault segment by the length of the segment in km.

1972] within all three Hill segments. Low ground and unconsolidated sediments are found in the intervening Canal and North Shore segments which are parallel, or near-parallel, to the N40±1W inferred plate slip vector [Minster and Jordan, 1978; Bird and Rosenstock, 1984] and to the direction of maximum shear strain inferred by Savage [1983]. We interpret the absence of transpression in the N40W and N44W segments to confirm the azimuth of local plate slip.

The near absence of triggered slip in the two segments closest in orientation to the inferred slip direction is puzzling. Moreover, the only creep measurement in these segments, at North Shore [Louie et al., 1985], indicates that no creep has occurred since 1968. Normal forces tending to increase frictional resistance are lowest in these segments, which should allow them to slip readily. A possible explanation, consistent with the poor expression of the fault in the Canal and North Shore segments and pronounced tilting across the fault at North Shore [Sharp, 1984], is that fault creep is distributed over a wide fault zone and has thereby escaped detection.

Transpression

If the surface geometry persists at depth, the Mecca and Durmid segments of the fault act as 1.6-km sawtooth indentations impeding fault movement. It is thus of considerable interest to establish whether transpression results from seismic slip or from interseismic deformation since this will affect earthquake prediction strategies in the region. Some idea of the rate of uplift of sediments with a transpressive segment of the fault is derived from an antecedent stream that cuts through Durmid Hill [Babcock, 1974]. If we assume that uplift of Durmid Hill (85 ± 15 m) and dextral offset of Salt Creek (850 m) by movement of the fault started at the same time (e.g., after peneplanation of a former Durmid Hill) we obtain a 10:1 ratio of slip to uplift. Using a fault slip rate [Keller et al., 1982] of 30 ± 6 mm/a, we estimate the age of Durmid Hill as 28 ± 6 ka, and its uplift rate to be 3 ± 1.2 mm/a. A youthful radial drainage pattern attests to the recent uplift of Durmid Hill and geodetic leveling data confirm localized current uplift (Figure 2(e)).

The difference between the plate slip azimuth and the strike of the fault through Durmid Hill is 7.5 ± 1 degrees. Thus the ratio of slip to compression across the fault is 8:1 and the amount of compression since peneplanation of the area is 106 ± 13 m. This yields an average strain rate of 0.75 μstrain/a for the last 28 ka assuming that the deformation is confined to the 5 km wide hill. The strain rate is consistent with the minimum 0.4 μstrain/a of compression derived from estimates of section shortening (30%) approximately normal to the fault evident within folded sediments of Pleistocene age (700 ka), exposed in the Durmid anticline [Fig. 8, Babcock, 1974]. A 1-km baseline trilateration network near Salt Creek (W. Prescott, personal communication 1985) indicates less than 0.1 μstrain/a in the past decade. The observed creep rate (≈2 mm/a) results in a possible instantaneous fault compression rate of 0.05 μstrain/a, consistent with the geodetic data. We conclude that fault-zone trans-

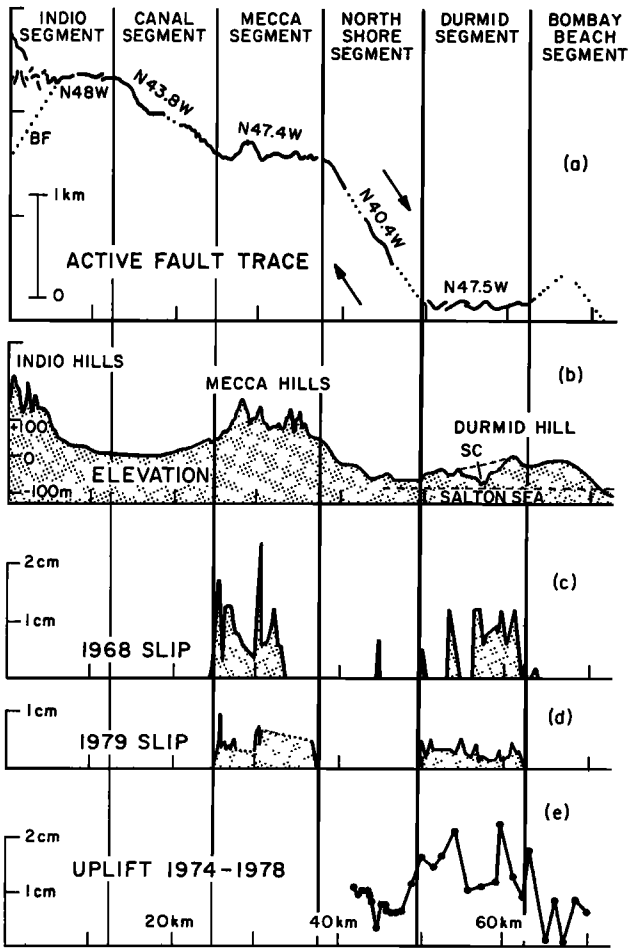

Fig. 2. (a) Map view of the southern San Andreas fault trace in the Coachella Valley exaggerated 12.5:1 normal to N47.5W strike. Vertical lines indicate bends between adjacent straight segments with the indicated angular values. The strike of the fault near Bombay Beach is uncertain. High ground (b) is associated with segments trending oblique to the inferred N40W plate slip vector (heavy arrows in (a)). Triggered slip is confined almost entirely to the Mecca and Durmid segments (c), (d). A geodetic leveling line along the NE Shore of the Salton Sea measured in 1974, 1976 and 1978 shows relative uplift near the segment that slipped in 1979 (e) although the signal is close to the noise level in the data. The line is associated with negligible refraction errors but a linear N-S trend, thought to be caused by a systematic magnetic effect in the leveling data, has been removed. SC = Salt Creek. BF = inferred location of Banning fault.

pression must be an intermittent process, perhaps occurring during earthquakes [cf. Yielding et al., 1981; Stein and King, 1984].

Conclusions

Simple geometric segmentation of the southernmost 72 km of the San Andreas fault with a characteristic segment length of ≈12.3 km determines the nature of seismic and aseismic deformation processes near the fault zone. A 7.5 degree angular difference between the plate slip vector and the local strike of the fault resulting in an 8:1 ratio of dextral slip to fault-zone compression, accounts for the transpressive features of the Indio, Mecca and Durmid Hills. Uplift of Durmid Hill appears to have occurred in the last 28 ± 6 ka at a rate of 3 ± 1 mm/a. The present creep rate is too low to generate this uplift rate or the inferred geologic rate of compression across the fault zone (0.75 μstrain/a), and it is possible that much of the observed deformation has occurred during earthquakes.

A large magnitude earthquake (M > 7.6) may be overdue on the southern San Andreas fault. According to the findings of King and Nabelek [1985] fault rupture typically propagates from a bend, to a bend. They suggest a possible earthquake prediction strategy might be to monitor interseismic deformation processes at bends. We have identified the location of six bends in the fault that could be considered areas for concentrated deformation monitoring. Moreover, the sawtooth geometry of the fault results in a characteristic strain field with dimensions of the order of 12 km, a scale that is poorly observable with current geodesy in the Coachella Valley. The study of the earthquake preparation process on the southern San Andreas fault would benefit considerably from the availability of tilt and strain data obtained near bends in the fault zone, and from <2-km baseline geodesy within 12 km of the fault.

Acknowledgments. We thank D. Agnew, M. Clarke, G. King, K. Sieh, A. Sylvester, L. Sykes, and M. Wyss for their critical comments on the results. L. Seeber and C. Scholz critically reviewed the manuscript and an anonymous reviewer offered several helpful improvements to the text. This work was supported by USGS contracts 21296 and 21918, NASA contract NA5-27237, and by the National Geophysical Data Service. Lamont Doherty Geological Observatory contribution number 3859.

References

Allen, C. R., M. Wyss, J. N. Brune, A. Granz, and R. Wallace, Displacements on the Imperial, Superstition Hills and San Andreas fault triggered by the Borrego Mountain Earthquake, in The Borrego Mountain Earthquake, U. S. Geological Survey Professional Paper 787, pp. 87-104, 1972.

Babcock, E. A., Geology of the NE margin of the Salton Trough, Salton Sea, California, Geol. Soc. Am. Bull., 85, 321-332, 1974.

Bird, P. and R. W. Rosenstock, Kinematics of present crust and mantle flow in southern California, Geol. Soc. Am. Bull., 95, 946-957, 1984.

Clark, M. M., Map showing recently active breaks of the San Andreas fault and associated faults between Salton Sea and Whitewater River, Mission Creek, California, Misc. Investigations Series, U. S. Geol. Soc. Map 1-1483, 1984.

Fuis, G. S. Displacement of the Superstition

Hills fault triggered by the earthquake, in The Imperial Valley Earthquake of October 15, 1979, U. S. Geological Survey Professional Paper 1254, pp. 145-153, 1972.

Keller, E. A., M. S. Bonkowski, R. J. Korsch, and R. J. Schlemon, Tectonic geomorphology of the San Andreas fault zone in the southern Indio Hills, Coachella Valley, California, Geol. Soc. Am. Bull., 93, 46-56, 1982.

King, G. C. P. and J. Nabelek, The role of bends in faults in the initiation and termination of earthquake rupture: Implications for earthquake prediction, Science, 228, 984-987, 1985.

King, N. E. and J. C. Savage, Strain rate profile across the Elsinore, San Jacinto and San Andreas faults near Palm Springs, California 1973-1981, Geophys. Res. Lett., 10, 55-57, 1983.

Louie, J. N., C. R. Allen, D. C. Johnson, P. C. Haase, and S. N. Cohn, Fault slip in southern California, Bull. Seism. Soc. Am., 75, 811-834, 1985.

Minster, J. B. and T. H. Jordan, Present day tectonic motions, J. Geophys. Res., 83, 5331-5354, 1978.

Sanderson, J. D. and W. R. D. Marchini, Transpression, J. Struct. Geol., 6, 449-458, 1984.

Savage, J. C., Strain accumulation in western United States, Ann. Rev. Earth Planet. Sci., 11, 11-43, 1983.

Sharp, R. V., Tectonic setting of the Salton Trough, in The Borrego Mountain Earthquake, U. S. Geological Survey Professional Paper 787, pp. 3-15, 1972.

Sharp, R. V., Salton Trough tectonics and quaternary Faulting, U. S. Geological Survey Open File Report 83-918, p. 133, 1984.

Sieh, K. E., Slip along the San Andreas fault associated with the earthquake, in The Imperial Valley Earthquake of October 15, 1979, U. S. Geological Survey Professional Paper 1254, pp. 155-160, 1982.

Stein, R. S. and G. C. P. King, Seismic potential revealed by surface folding: 1983 Coalinga earthquake, Science, 224, 869-872, 1984.

Sylvester, A. G. and R. R. Smith, Tectonic transpression and basement controlled deformation in the San Andreas fault zone, Salton Trough, California, Am. Assoc. Petrol. Geol. Bull., 60, 2081-2101, 1976.

Sykes, L. R. and S. P. Nishenko, Probabilities of occurrence of large earthquakes on the San Andreas, San Jacinto and Imperial faults, California, 1823-2003, J. Geophys. Res., 89, 5905-5927, 1984.

Wallace, R. E., Surface fracture patterns along the San Andreas Fault, in Proc. Conf. on Tectonic Problems of the San Andreas Fault System, Stanford Univ. Pub. Geol. Sci. 13, 248-250, 1973.

Yielding, G., J. A. Jackson, G. C. P. King, H. Sinvhal, C. Vita-Finzi and R. M. Wood, Relations between surface deformation, fault geometry, seismicity and rupture characteristics during the El Asnam (Algeria) Earthquake of October 10, 1980, Earth Planet. Sci. Lett., 56, 287-304, 1981.

Roger Bilham and Patrick Williams, Lamont-Doherty Geological Observatory, Columbia University, Palisades, NY 10964.

(Received June 20, 1985;
accepted July 5, 1985)